Torque Ripple Suppression Of SRM Using Sliding Mode Current Compensation

Qin Li[1], Benqin Jing[2*], Peiming Luo[1], and Xuexi Zhang[1]

[1] School of Automation ,Guangdong University of Technology, Guangzhou, China
[2] School of Electronic Information and Automation, Guilin University of Aerospace Technology, Guilin, China
[*] Corresponding author. E-mail: jingbenqin@guat.edu.cn

Received: May 05, 2023; Accepted: Aug. 22, 2023

Switched Reluctance Motor (SRM) implement is constrained by high torque ripple. An effective torque ripple compensation method is proposed based on sliding mode current compensation (SMCC). According to the relationship between torque and current of the SRM, a current compensation with a sliding mode controller is designed. The input of the sliding mode controller is the difference between the reference torque and instant torque, and the compensation current is obtained as the output through the calculation of the sliding mode surface. The total current is the sum of linear conversion current and compensation current. The Lyapunov stability criterion proves the stability of the sliding mode compensation. In MATLAB simulation environment and low-speed operation of the motor, the effectiveness of the proposed method is proved. Compared with PD current compensation method, the efficiency of this method in current compensation is improved, and the torque ripple can be effectively reduced.

Keywords: SRM; Torque Ripple; PD Algorithm; Sliding mode control; Current profiling control

http://dx.doi.org/10.6180/jase.202406_27(6).0004

1. Introduction

In the field of new energy vehicles, Switched Reluctance Motor (SRM) with excellent performance such as high reliability, extensive speed range, and no need for rare metal manufacturing have attracted increased attention. However, due to its unique doubly salient structure and magnetic saturation operation characteristics, large torque ripple will occur during the middle and low-speed operation [1, 2]. Therefore, researchers have conducted lots of research on torque ripple [3].

Methods for suppressing torque ripple include: direct torque control (DTC), model predictive control (MPC) and current control [4]. The DTC method evolved from asynchronous motors, and its control method requires both estimated torque and estimated flux, which requires a large amount of computation. The MPC method estimates the control quantity based on the model, which requires high accuracy of the model [5]. Thanks to the current control in SRM, the electromagnetic torque is relatively stable during low-speed operation. Traditional current control methods include the torque sharing function (TSF) method, harmonic current injection method, and current profile control method [6]. The torque distribution method generates the reference torque and then assigns the reference torque to the phase current according to the formula $i(T,\theta)$. Since torque is a strong nonlinear function of current and position, the TSF used significantly impacts torque control performance. To improve the implementation of SRM, the distribution function of TSF needs to improve [7–10]. The turn-on angle and overlap angle in SRM significantly impact their performance. Therefore, a genetic algorithm is used to optimize the turn-on angle and overlap angles under different expected torque requirements [7]. As the current hysteresis impacts the torque ripple of SRM, the current shaping control designed according to the rotor

angle reduce the torque ripple [11]. As the current is affected by the TSF method, the torque ripple performance of SRM can be improved by adjusting the weight parameter used to calculate the current percentage of the output phase [12]. Furthermore, considering the difference between instant and estimated torque, a new TSF method is proposed, which uses predictive model control to effectively compensate for the insufficient capacity of the incoming phase in TSF [13]. By obtaining the range of phase torque and applying it to online correction of reference phase torque, torque ripple can also be reduced [14]. In general, the TSF method can reduce the torque ripple of SRM, but rely on the precise TSF formula. The harmonic current injection method fully considers the periodicity of the current and inductance distribution in the steady state [15]. The average torque is mainly contributed by DC, primary and secondary harmonics, while the fourth and fifth harmonics significantly affect torque ripple. The torque performance can be improved by actively and selectively injecting current harmonics [16]. By superposing the first five current harmonics of the opti- mum amplitude and phase on the rectangular current reference, it is possible to significantly improve the torque control performance in the low-speed region [17]. The optimum current harmonics can be found online using the simplex approach, and this method can be further expanded to the high-speed range [18]. The current reference based on half sine wave can also suppress torque ripple [19]. The torque and radial force ripple can be reduced simultaneously by determining appropriate current harmonic optimization through numerical calculation[20, 21].

The current profile control method is another practical indirect method for determining the reference current directly. Generally, the current control starts with a simple reference current and then fine tune as needed to obtain the final reference current with suitable torque control performance. As the bus current influences torque, the negative part of the bus current and commutation shift technology can be used to form a standard rectangular reference current[22]. The feed-forward plus torque compensation can reduce the dynamic response time and improve the steady-state accuracy of electromagnetic torque [23].

The other methods widely used in SRM include fuzzy control and neural network control. The torque ripple can be suppressed by designing appropriate fuzzy logic to optimize the segmented harmonic current online and by segmenting the harmonic current [24]. The fuzzy control depends on the establishment of its fuzzy rules, which is time-consuming. Neural network control has disadvantages such as large amount of calculation, lack of strict mathematical proof of control stability, its use requires offline training in advance in most cases [25, 26].

Sliding mode control (SMC) and its improved method have been used in SRM speed regulation control. However, at present, there is no literature that applies sliding mode control to current compensation. The sliding mode surface according to the mechanical equation of the motor, and the sliding mode surface needs to be stable so that the system has strong robustness to uncertain parameters and external disturbances. None literature applies sliding mode control to current compensation control at present. The difficulty lies in designing the sliding mode surface of compensation current according to the relationship equation between torque and current and the design need to be stability. The advantages of sliding mode control include fast dynamic response, low computational complexity, and good stability assurance.

The innovation of this paper is the design of a sliding mode current compensation (SMCC) based on torque error. The sliding mode surface is designed based on the relationship between torque error and compensation current, and together with the feed-forward current conversion, it generates a total current with low computational complexity and fast response speed. Finally, the stability of the sliding mode controller is proven. The algorithm can effectively reduce torque ripple and has low computation. It can meet the demand for an onboard controller for the SRM drive.

The remainder of this manuscript is organized as follows. Section 2 presents the principle of indirect torque control. The proposed SMCC is descripted in Section 3. To verify the effectiveness of SMCC, simulation results and analysis are provided in Section 4, followed by the conclusion in Section 5.

2. Indirect torque control

According to the mechanical equation of SRM, the relationship between magnetic co-energy and phase current is

$$W_{\mathrm{m}}(i,\theta) = W_{\mathrm{m}}^{*}(i,\theta) = \frac{1}{2}\mathrm{i}\psi = \frac{1}{2}Li^{2} \tag{1}$$

where W_{m} is the magnetic co-energy, ψ is the flux linkage, i is the phase current, and L is the inductance.

Thus, the electromagnetic torque equation becomes

$$T_{\mathrm{e}}(i,\theta) = \frac{1}{2}\mathrm{i}^{2}\frac{\partial L}{\partial \theta} \tag{2}$$

It can be further obtained that the current calculation formula is

$$i = \sqrt{\frac{2T_{e}}{\partial L/\partial \theta}} \tag{3}$$

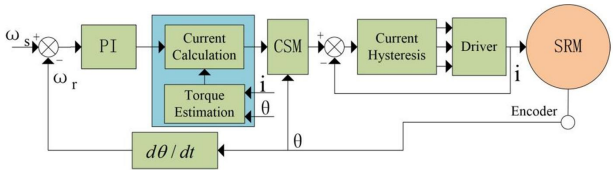

Fig. 1. Indirect torque control

Therefore, the reference torque is obtained. Treating the inductance deflection as linearized, the total reference current can be calculated according to Eq. (3), and the structure of the control system formed is shown in Fig. 1. The system is a double closed-loop control structure. The inner loop is a current loop, and the outer loop is a speed loop.

Torque estimation is obtained by looking up the torque table, which is established using the locked rotor method. This involves fixing the rotor at different rotor angles, applying different current values, measuring the output torque every time, and recording the data. Repeat the process to obtain a set of torque data and store it in the torque table. During SRM operation, the rotor angle and current are queried in real-time to obtain the electromagnetic torque, which is the estimated torque.

The torque estimation and the reference torque are used to calculate the total current. As the total current is obtained, the total current is distributed according to the rotor angle. The current hysteresis comprises the reference current and the feedback current. The hysteresis calculation results are used to drive the circuit on and off. The current distribution is based on the total reference current and the rotor angle. The expected current of each phase winding at any rotor angle is calculated in real-time. According to the distribution algorithm, each phase's current value is obtained. At the same time, the sum of the given current of each phase is constant, controlling the current and suppressing torque ripple. At any time during the operation of the motor, one or two phases are turned on, which satisfy Eq. (4).

$$\begin{cases} i_{\mathrm{k}}(\theta) = i_{\mathrm{all}}\, f_k(\theta) & k = 1,2,3,\ldots,m \\ \sum_{k=1}^{m} f_k(\theta) = 1 & 0 \le f_k(\theta) \le 1 \end{cases} \tag{4}$$

Where i_{all} is the total reference current, i_k is the reference k-phase current, and f_k is the current distribution function.

The current sharing method (CSM) is employed to ensure the sum of the total current maintaining a constant value according to the rotor angle, therefore, it is necessary to reasonably design the current distribution function. In the control system based on torque distribution function, typical torque distribution methods include linear, sinusoidal, and cubic torque distribution methods. Among them, the effect of the transition section in the cubic torque distribution method is stable. Regarding these method, the cubic current distribution method is chosen, and its distribution function is shown in Eq. (5).

$$f_k(\theta) = \begin{cases} 0 & 0 \le \theta < \theta_{\mathrm{on}} \\ 3\left(\frac{\theta-\theta_{\mathrm{on}}}{\theta_{\mathrm{or}}}\right)^2 - 2\left(\frac{\theta-\theta_{\mathrm{on}}}{\theta_{\mathrm{or}}}\right)^3 & \theta_{\mathrm{on}} \le \theta < \theta_{\mathrm{on}} + \theta_{\mathrm{or}} \\ 1 & \theta_{\mathrm{on}} + \theta_{\mathrm{or}} \le \theta < \theta_{\mathrm{off}} \\ 1 - 3\left(\frac{\theta-\theta_{\mathrm{off}}}{\theta_{\mathrm{or}}}\right)^2 + 2\left(\frac{\theta-\theta_{\mathrm{of}}}{\theta_{\mathrm{or}}}\right)^3 & \theta_{\mathrm{orf}} \le \theta \le \theta_{\mathrm{off}} + \theta_{\mathrm{or}} \\ 0 & \theta_{\mathrm{off}} + \theta_{\mathrm{or}} \le \theta \le \tau_t \end{cases} \tag{5}$$

where θ_{on} is the turn on angle, θ_{off} is the turn off angle, θ_{or} the overlap angle, and τ_t is the period.

The hysteresis current compares the phase current with the reference phase current to obtain the state of the driving signal. If the state is "-1", the output is turned off, if the state is " 0", the driving circuit is half on for continuous current, and if the state is " 1 ", the power supply is turned on. The calculation formula for current hysteresis loop is

$$sig = \begin{cases} -1, & i > I_{\max} \\ 0, & I_{\min} < i < I_{\max} \\ 1, & i < I_{\min} \end{cases} \tag{6}$$

where sig is the drive signal, i is the phase current, $i_{\max}$ is the maximum chop current, and $i_{\min}$ is the minimum chop current.

3. Current profiling in srm

The smooth commutation of SRM is the critical factor for its stable operation. During commutation, the power supply of the outgoing phase is turned off, the phase current gradually decreases, and the electromagnetic torque decreases. At the same time, the incoming phase is turned on, the phase current gradually increases, and the electromagnetic torque increases. The total electromagnetic torque is the sum of the electromagnetic torque of the previous phase and the latter phases' electromagnetic torque. The goal of designing the current distribution function is to make the torque increase by the incoming phase just offset the decrease caused by the outgoing phase. Therefore, the total electromagnetic torque remains constant.

The indirect torque control method achieves the stable operation of the SRM and constant electromagnetic torque by controlling the current. According to the torque current conversion relationship, the inductance derivative can be

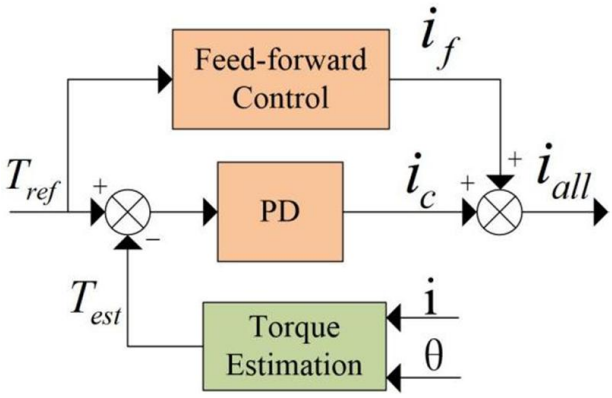

Fig. 2. PD current compensation

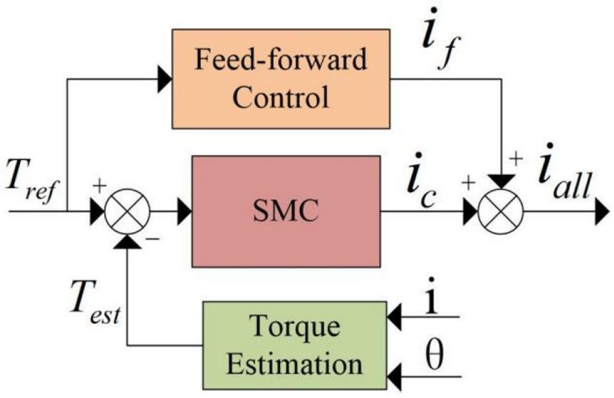

Fig. 3. SMCC control

linearized and the resulting errors can be handled by the proportion differential (PD) algorithm. A typical control structure based on PD current compensation is shown in Fig. 2.

The feed-forward controller generates a current based on the linearized reference torque. With the set speed unchanged, the reference torque value is maintained constant through the PI speed controller. Therefore, the generated linear current is a constant value, which cannot meet the current requirements at different rotor angles, causing torque ripple. When the reference torque increases or decreases, the linear current output of the feed-forward controller will correspondingly increase or decrease. The PD current compensation is used to calculate the compensation current according to the difference between the reference torque and the instant torque, that is, the torque error. If the torque error is negative, the instant torque is too large. And the PD calculation generate negative compensation current and reduces the output current to reduce the electromagnetic torque. On the contrary, if the torque error is positive, the instant torque is too small. Then, the PD calculation generate positive compensation current, increases the output current to increase the electromagnetic torque and finally achieves the goal of stable electromagnetic torque. The advantages of PD compensation method include simple control principle, easy implementation, simple parameter selection, and convenient parameter adjustment.

Unlike the proportion integral differential (PID) structure used for stability control under normal circumstances, the current controller needs the controller to respond to the change of torque error in real-time and output compensation current according to torque error.Therefore, the controller removes integral coefficient, thus forming the PD controller. The PD controller is discrete, and the calculation formula is

$$i_c = K_p * \Delta T(k) + K_d * [\Delta T(k) - \Delta T(k-1)] \quad (7)$$

Where i_c is the compensation current, $\Delta T(k)$ and $\Delta T(k-1)$ are the torque errors at time k and k − 1, respectively, k_p and k_d are proportional and differential coefficients.

The feed-forward controller, which converts the reference torque into the reference current according to Eq. (3). The feed-forward controller and PD current compensator work together to calculate the total current for the SRM drive system. PD controller is a model-free control method. Therefore, the system can achieve an acceptable control effect by adjusting its parameters to appropriate values. However, parameter adjustment often consumes too much time and is more sensitive to external interference. Extensive interference in the control process often causes instability in the system.

4. Smcc

4.1. Sliding mode compensator

The SMC controller is designed according to the mechanical equation of the motor and the relationship between torque and current. The reference torque, instant torque, and their difference are inputs of the sliding mode current compensator. The SMC control structure thus formed as shown in Fig. 3.

SMC is responsible for calculating the compensation current based on the magnitude of torque error. The sum of the compensation current and the linear transformation current forms the current profile. When the given speed remains constant, the reference torque value remains relatively constant. Then, SMC compensates the current profile based on the difference between the feedback torque and the reference torque. A positive torque error indicates

that the total current is insufficient and SMC increases the compensation current. Conversely, a negative torque error indicates that the total current is too large and SMC reduces the compensation current.

According to the torque generation Eq. (2), linearize the inductance partial conductance to 1, and we get

$$T = \frac{1}{2}i^2 \tag{8}$$

Setting the output of the sliding mode controller as i_c, calculate the derivative of i_c, then we have

$$\begin{cases} T = \frac{1}{2}i_c^2 \\ T' = i_c \end{cases} \tag{9}$$

The second derivative of torque is

$$\ddot{T} = \dot{i}_c = 1 \tag{10}$$

At the same time, the torque error is

$$e = \Delta T = T_{\text{ref}} - T_{\text{est}} \tag{11}$$

where ΔT, T_{ref} and T_{est} are the torque difference, reference torque and the instant torque respectively.

In the slide mode control, the design of sliding mode surfaces is the core of sliding mode control algorithms. The designed sliding mode surfaces need to enable the system to converge from any initial state to the sliding mode surface, and ultimately the system slides on the sliding mode surface to reach the system equilibrium point. The design sliding surface is

$$\begin{aligned} s &= ce + \dot{e} \\ &= c\left(T_{\text{ref}} - T_{\text{est}}\right) + \left(\dot{T}_{\text{ref}} - \dot{T}_{\text{est}}\right) \\ &= c\left(T_{\text{ref}} - T_{\text{est}}\right) - i_c \end{aligned} \tag{12}$$

calculate the derivative of s , then we can get

$$\begin{aligned} \dot{s} &= c\left(\dot{T}_{\text{ref}} - \dot{T}_{est}\right) - \dot{i}_c \\ &= -c * \dot{T}_{est} - 1 \\ &= -c * i_c - 1 \end{aligned} \tag{13}$$

where c is the scale factor and i_c is the compensation current. The sliding mode approach law is selected as

$$\dot{s} = -\varepsilon * \text{sign}(s) - k * s \tag{14}$$

where ε and k are positive real number, sign is a symbolic function, and its expression is

$$\text{sign}(s) = \begin{cases} -1, & s < 0 \\ 0, & s = 0 \\ 1, & s > 0 \end{cases} \tag{15}$$

combining Eqs. (13) and (14), then

$$-c * i_c - 1 = -\varepsilon * \text{sign}(s) - k * s \tag{16}$$

Then the output of the sliding mode controller is

$$i_c = \frac{1}{c}(\varepsilon * \text{sign}(s) + k * s - 1) \tag{17}$$

Among them, the scale factor c is used to adjust the proportion of compensation current, the constant velocity approach factor is used to adjust the approach time when s is close to zero, and the exponential approach factor is used to reduce the time of reaching the switching surface.

4.2. Stability analysis

Based on Lyapunov stability principle, the designed sliding mode stability criterion is

$$s * \dot{s} = s * (-\varepsilon * \text{sign}(s) - k * s) \tag{18}$$

The analysis under different conditions is as follows

when $s < 0$, then $-\varepsilon * \text{sign}(s) - k * s > 0$, therefore, $s * \dot{s} < 0$, when $s > 0$, then $-\varepsilon * \text{sign}(s) - k * s < 0$, therefore, $s * \dot{s} < 0$, when $s = 0$, then $-\varepsilon * \text{sign}(s) - k * s = 0$, therefore, $s * \dot{s} = 0$.

Therefore, The formula $s * \dot{s} \leq 0$ is always valid. According to the Lyapunov stability principle, the sliding mode control is in a stable state in any case, and the calculated sliding mode compensation current will make the system enter a stable state.

5. Simulation verification and analysis

To verify the feasibility of the SMCC, the simulation environment is established in the MATLAB environment. The SRM model is selected as three-phase 12/8 type. The results are compared with the PD current compensation method. The torque ripple coefficient used to evaluate torque ripple is defined as

$$T_{\text{rip}} = \frac{T_{\max} - T_{\min}}{T_{\text{ave}}} \times 100\% \tag{19}$$

where T_{rip} is torque ripple, $T_{\max}$ is maximum torque during the measuring circle, $T_{\min}$ is minimum torque during the measuring circle, T_{ave} is average torque during the measuring circle.

The parameters selected during the experiment are as follows. The number of stator poles is 12 , the number of rotor poles is 8 , the DC bus voltage is 60 V, the moment of inertia is 0.0082 kg $\cdot$ m^2, the friction coefficient is 0.01 N $\cdot$ m $\cdot$ s, and the set simulation time is 0.2 s. In the PD controller used for comparison, the parameter selection is $K_p = 6$ and $K_d = 0.6$ respectively, and the parameter selection of sliding mode controller is $c = 1, \varepsilon = 5$ and $k = 0.5$.

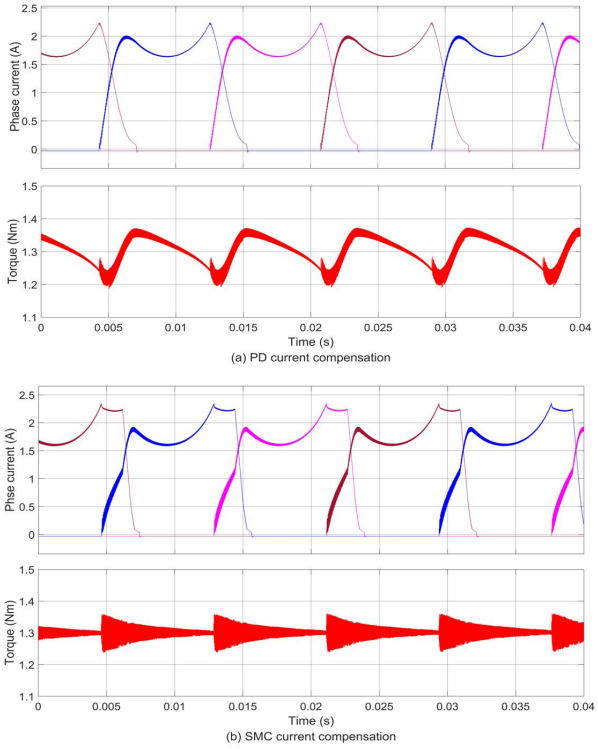

Fig. 4. Comparison of experimental results of load 1Nm and speed 300r/min

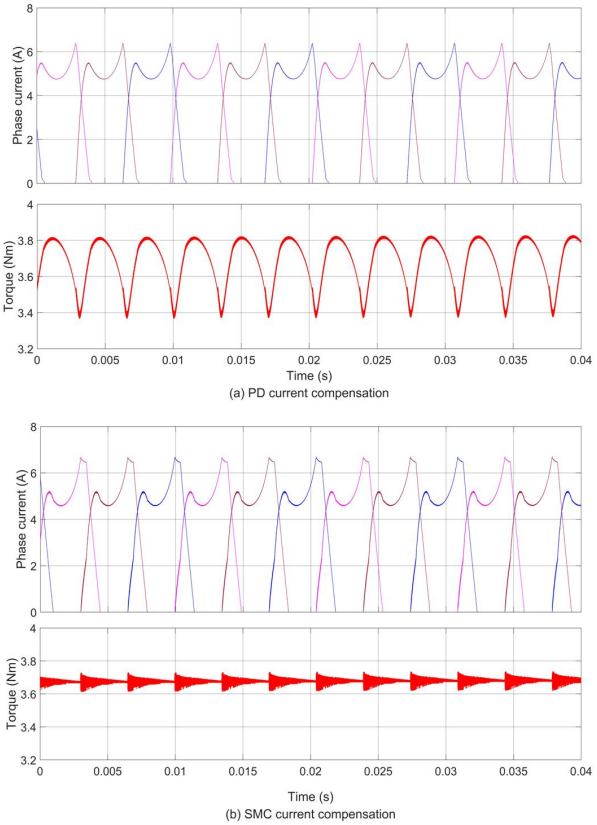

Fig. 5. Comparison of experimental results of load 3Nm and speed 700r/min

As the current hysteresis control method is more effective when the SRM operates at low speeds, the motor speed during simulation is set to low speed. The load torque is set as 1Nm, and the speed is 300r/min in the experiment. Observe the phase current and torque ripple with the two methods. Fig. 4 shows the waveform of phase current and electromagnetic torque of different current compensation methods when the speed is 300r/min, and the load torque is 1Nm. The torque ripple mainly occurs in the commutation process. In the commutation process, restraining torque ripple can be achieved by changing the waveform of phase current through adequate current compensation. At the same time, it can be seen from the current curve that the SMCC method reduces the current peak value of the turn-off phase at the beginning of the commutation and changes the current rise curvature of the incoming phase, which can more effectively reduce the torque ripple. As a result, the torque ripple of PD current compensation is 14.1%, while the torque ripple of SMCC is 9.3%,

To better verify the proposed method's reliability at low speeds, set the load torque to 3Nm and the speed to 700r/min, and obtain the phase current and torque wave forms under the PD current compensation control structure, as shown in Fig. 5. Due to the limited compensation ability of the PD control algorithm for current, the current cannot be quickly adjusted to the output current required for stable torque, and a large torque ripple still appears during commutation. Calculating by Eq. (19), it is found that the torque ripple of PD current compensation is 12.3%. However, the SMCC method, based on the sliding mode control method designed by torque error, can quickly adjust the compensation current, thereby changing the phase current and effectively reducing torque ripple. As a result, the torque ripple is reduced to 3.6%.

To comprehensively compare the torque ripple suppression ability of the proposed SMC current compensation method with the PD current compensation methods, the speed was set from 200r/min to 800r/min with an interval of 100r/min, and the load torques were set as 1Nm, 3Nm, and 5Nm, respectively. As a result, the torque ripple curves obtained by testing the SRM are shown as Figs. 6 to 8. It can be observed that as the torque increases, the torque ripple of both methods decreases. For example, at 700r/min, the torque ripple rates with the PD compensation are 14.5% and 12.3% at 1Nm and 3NM, respectively, while the torque ripple rates with the SMC compensation are 7.5% and 3.6%

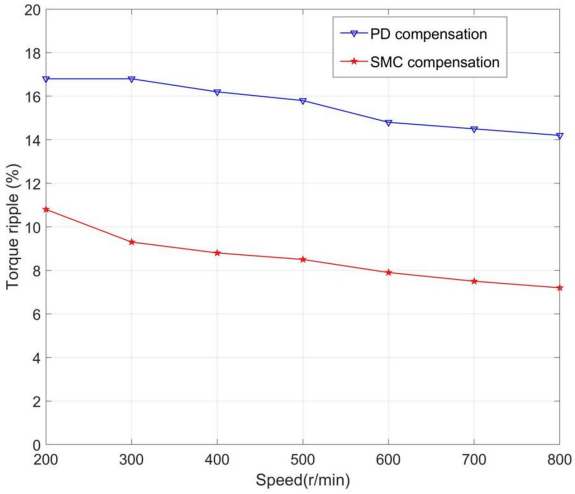

Fig. 6. Comparison of experimental results with different speed under load 1Nm

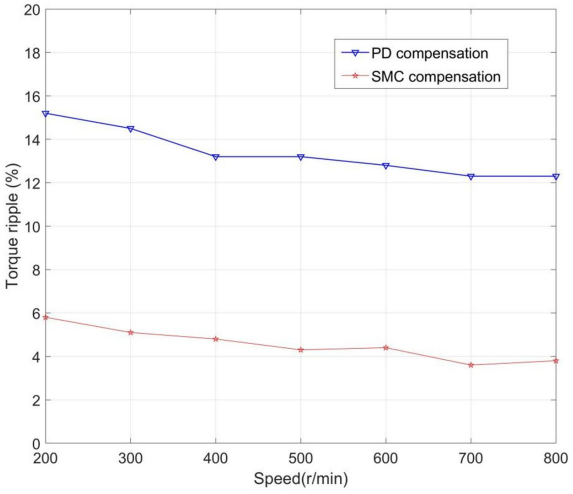

Fig. 7. Comparison of experimental results with different speed under load 3Nm

at 1Nm and 3NM, respectively. The torque ripple with the SMC compensation decreases more. Due to the reason that the increase of electromagnetic torque result in the increases of current. With the action of the current hysteresis controller, the upper and lower limits of torque ripple can be controlled to a certain range. According to Eq. (19), when the average torque increases, the torque ripple will decrease.

The comparison under different speeds and load conditions shows that the SMCC method can effectively reduce torque ripple in middle and low-speed situations. However, with the load increase, the sliding mode compensation control method has more evident advantages at suppressing torque ripple.

6. Conclusion

This paper proposes a torque ripple suppression method of SMCC under indirect torque control strategy. Compared with the PD current compensation method, the proposed method effectively reduces the torque ripple under different torque load and speeds. The main improvement points are as follows:

1. To obtain a stable electromagnetic torque, a quickly current compensate is essential. A control structure is designed by combining the linear feed-forward current with the nonlinear SMCC, with fully considering the nonlinear relationship of the electromagnetic torque and current.

2. According to the conversion equation of torque to current, the sliding mode current compensator is designed, and sliding mode surface and reaching law can ensure the system stable. The Lyapunov stability criterion can prove the stability of the designed compensator.

3. With the minimum torque ripple as the control objective, different load torques and speeds are tested at low speeds and compared with the conventional PD current compensation method to verify the effectiveness of the proposed SMCC method.

Acknowledgment

This work was financially supported partly by the National Natural Science Foundation of China under Grant 62263004 and Grant 62263009.

References

[1] C. Gan, J. Wu, Q. Sun, W. Kong, H. Li, and Y. Hu, (2018) *"A review on machine topologies and control techniques for low-noise switched reluctance motors in electric vehicle applications"* **IEEE Access** *6*: 31430–31443. DOI: 10.1109/ACCESS.2018.2837111.

[2] E. Bostanci, M. Moallem, A. Parsapour, and B. Fahimi, (2017) *"Opportunities and challenges of switched reluctance motor drives for electric propulsion: A comparative study"* **IEEE transactions on transportation electrification** *3*(1): 58–75. DOI: 10.1109/TTE.2017.2649883.

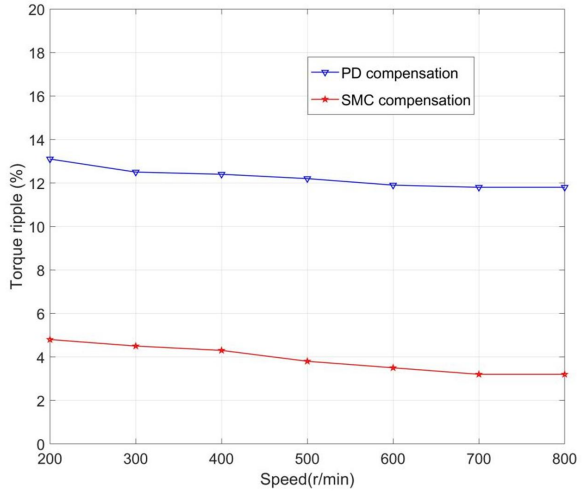

Fig. 8. Comparison of experimental results with different speed under load 5Nm

[3] J.-W. Ahn and G. F. Lukman, (2018) *"Switched reluctance motor: Research trends and overview"* **CES Transactions on Electrical Machines and Systems** *2*(4): 339–347.

[4] D. Mohanraj, J. Gopalakrishnan, B. Chokkalingam, and L. Mihet-Popa, (2022) *"Critical Aspects of Electric Motor Drive Controllers and Mitigation of Torque Ripple-Review"* **IEEE Access**: DOI: 10.1109/ACCESS.2022.3187515.

[5] M. Deepak, G. Janaki, and C. Bharatiraja, (2022) *"Power electronic converter topologies for switched reluctance motor towards torque ripple analysis"* **Materials Today: Proceedings** *52*: 1657–1665. DOI: 10.1016/j.matpr.2021.11.284.

[6] G. Fang, F. P. Scalcon, D. Xiao, R. P. Vieira, H. A. Gründling, and A. Emadi, (2021) *"Advanced control of switched reluctance motors (SRMs): A review on current regulation, torque control and vibration suppression"* **IEEE Open Journal of the Industrial Electronics Society 2**: 280–301.

[7] X. Xue, K. W. E. Cheng, and S. L. Ho, (2009) *"Optimization and evaluation of torque-sharing functions for torque ripple minimization in switched reluctance motor drives"* **IEEE transactions on power electronics** *24*(9): 2076–2090. DOI: 10.1109/TPEL.2009.2019581.

[8] J. Ye, B. Bilgin, and A. Emadi, (2015) *"An offline torque sharing function for torque ripple reduction in switched reluctance motor drives"* **IEEE Transactions on energy conversion** *30*(2): 726–735. DOI: 10.1109/TEC.2014.2383991.

[9] D.-H. Lee, J. Liang, Z.-G. Lee, and J.-W. Ahn, (2009) *"A simple nonlinear logical torque sharing function for low-torque ripple SR drive"* **IEEE Transactions on Industrial Electronics** *56*(8): 3021–3028. DOI: 10.1109/TIE.2009.2024661.

[10] S. K. Sahoo, S. K. Panda, and J.-X. Xu, (2005) *"Indirect torque control of switched reluctance motors using iterative learning control"* **IEEE Transactions on Power Electronics** *20*(1): 200–208. DOI: 10.1109/TPEL.2004.839807.

[11] H.-H. Lee, Q. Wang, S.-J. Kim, W. Choi, and G.-H. Lee, (2012) *"A Simplified torque ripple reduction using the current shaping of the flux switched reluctance motor"* **Journal of Magnetics** *17*(3): 200–205. DOI: 10.4283/JMAG.2012.17.3.200.

[12] H. Li, B. Bilgin, and A. Emadi, (2018) *"An improved torque sharing function for torque ripple reduction in switched reluctance machines"* **IEEE Transactions on Power Electronics** *34*(2): 1635–1644. DOI: 10.1109/TPEL.2018.2835773.

[13] S. Song, R. Hei, R. Ma, and W. Liu, (2020) *"Model predictive control of switched reluctance starter/generator with torque sharing and compensation"* **IEEE Transactions on Transportation Electrification** *6*(4): 1519–1527. DOI: 10.1109/TTE.2020.2975908.

[14] S. Song, S. Huang, Y. Zhao, X. Zhao, X. Duan, R. Ma, and W. Liu, (2022) *"Torque Ripple Reduction of Switched Reluctance Machine With Torque Distribution and Online Correction"* **IEEE Transactions on Industrial Electronics** *70*(9): 8842–8852. DOI: 10.1109/TIE.2022.3210516.

[15] Z. Zhu, B. Lee, L. Huang, and W. Chu, (2016) *"Contribution of current harmonics to average torque and torque ripple in switched reluctance machines"* **IEEE Transactions on magnetics** *53*(3): 1–9. DOI: 10.1109/TMAG.2016.2633477.

[16] X. Liu, Z. Zhu, and Z. Pan. "Analysis of electromagnetic torque in sinusoidal excited switched reluctance machines having DC bias in excitation". In: *2012 XXth International Conference on Electrical Machines*. IEEE. 2012, 2882–2888. DOI: 10.1109/ICElMach.2012.6350296.

[17] J. Stephenson, A. Hughes, and R. Mann, (2001) *"Torque ripple minimisation in a switched reluctance motor by optimum harmonic current injection"* **IEE Proceedings-Electric Power Applications** *148*(4): 322–328. DOI: 10.1049/ip-epa:20010480.

[18] J. Stephenson, A. Hughes, and R. Mann, (2002) *"Online torque-ripple minimisation in a switched reluctance motor over a wide speed range"* **IEE Proceedings-Electric Power Applications *149***(4): 261–267. DOI: 10.1049/ip-epa:20020373.

[19] N. T. Shaked and R. Rabinovici, (2005) *"New procedures for minimizing the torque ripple in switched reluctance motors by optimizing the phase-current profile"* **IEEE Transactions on magnetics *41***(3): 1184–1192. DOI: 10.1109/TMAG.2004.843311.

[20] C. Ma, L. Qu, R. Mitra, P. Pramod, and R. Islam. "Vibration and torque ripple reduction of switched reluctance motors through current profile optimization". In: *2016 IEEE Applied Power Electronics Conference and Exposition (APEC)*. IEEE. 2016, 3279–3285. DOI: 10.1109/APEC.2016.7468336.

[21] O. Gundogmus, Y. Sozer, L. Vadamodala, J. Kutz, J. Tylenda, and R. L. Wright. "Current harmonics injection method for simultaneous torque and radial force ripple mitigation to reduce acoustic noise and vibration in SRMs". In: *2019 IEEE Energy Conversion Congress and Exposition (ECCE)*. IEEE. 2019, 7091–7097. DOI: 10.1109/ECCE.2019.8913056.

[22] J. Chai and C. Liaw, (2010) *"Reduction of speed ripple and vibration for switched reluctance motor drive via intelligent current profiling"* **IET Electric Power Applications *4***(5): 380–396. DOI: 10.1049/iet-epa.2009.0061.

[23] H. Cheng, H. Chen, Z. Yang, and W. Huang, (2015) *"Braking torque closed-loop control of switched reluctance machines for electric vehicles"* **Journal of Power Electronics *15***(2): 469–478. DOI: 10.6113/JPE.2015.15.2.469.

[24] M. Ma, F. Ling, F. Li, and F. Liu, (2020) *"Torque ripple suppression of switched reluctance motor by segmented harmonic currents injection based on adaptive fuzzy logic control"* **IET Electric Power Applications *14***(2): 325–335. DOI: 10.1049/iet-epa.2019.0027.

[25] M. Deepak, G. Janaki, and C. Bharatiraja. "A Mathematical Modelling Approach Switched Reluctance Motor for Low Speed torque ripple minimization by Sensorless Intelligent Control". In: *2023 IEEE IAS Global Conference on Renewable Energy and Hydrogen Technologies (GlobConHT)*. IEEE. 2023, 1–6. DOI: 10.1109/GlobConHT56829.2023.10087413.

[26] M. Deepak, G. Janaki, C. Bharatiraja, et al., (2022) *"Design Switched Reluctance Motor Rotor Modification Towards Torque Ripple Analysis For EVs"* **Journal of Applied Science and Engineering *26***(7): 949–958. DOI: 10.6180/jase.202307_26(7).0006.